- ORIGINAL ARTICLE -

Effective Smoke Detection Using Spatial-Temporal Energy and Weber Local Descriptors in Three Orthogonal Planes (WLD-TOP)

John Adedapo Ojo[1], Jamiu Alabi Oladosu [2]

[1] *Department of Electronic & Electrical Engineering, Ladoke Akintola University of Technology, P.M.B 4000, Ogbomoso, Nigeria.*
jaojo@lautech.edu.ng
[2] *Department of Electronic & Electrical Engineering, Ladoke Akintola University of Technology, P.M.B 4000, Ogbomoso, Nigeria.*
ola_dosu1@yahoo.com

Abstract

Video-based fire detection (VFD) technologies have received significant attention from both academic and industrial communities recently. However, existing VFD approaches are still susceptible to false alarms due to changes in illumination, camera noise, variability of shape, motion, colour, irregular patterns of smoke and flames, modelling and training inaccuracies. Hence, this work aimed at developing a VSD system that will have a high detection rate, low false-alarm rate and short response time. Moving blocks in video frames were segmented and analysed in HSI colour space, and wavelet energy analysis of the smoke candidate blocks was performed. In addition, Dynamic texture descriptors were obtained using Weber Local Descriptor in Three Orthogonal Planes (WLD-TOP). These features were combined and used as inputs to Support Vector Classifier with radial based kernel function, while post-processing stage employs temporal image filtering to reduce false alarm. The algorithm was implemented in MATLAB 8.1.0.604 (R2013a). Accuracy of 99.30%, detection rate of 99.28% and false alarm rate of 0.65% were obtained when tested with some online videos. The output of this work would find applications in early fire detection systems and other applications such as robot vision and automated inspection.

Keywords: Video-based smoke detection, Weber Local Descriptor, Three Orthogonal Planes, Dynamic texture descriptors, Support Vector Machine.

Citation: J. A. Ojo and J. A. Oladosu. "*Effective Smoke Detection Using Spatial-Temporal Energy and Weber Local Descriptors in Three Orthogonal Planes (WLD-TOP",* Journal of Computer Science & Technology, vol. 18, no. 1, pp.35-47, 2018.

DOI: 10.24215/16666038.18.e05

Received: July 4, 2017 **Revised:** December 04, 2017 & February 07, 2018 **Accepted:** February 15, 2018

Copyright: This article is distributed under the terms of the Creative Commons License CC-BY-NC.

1. Introduction

Fire is one of the major hazards of the modern society as it causes grave and significant losses of lives, properties and socio-economic infrastructures around the world every year. In the past decades, different technologies have been developed to detect and control fire at very early stage. These technologies can be broadly classified into conventional methods and video-based techniques. Conventional methods employ ion or particle sensors, heat sensors, optical sensors (infrared, visible, ultraviolet), relative humidity sampler or air transparency sampler; whereas video-based fire detection (VFD) systems use video camera and computational techniques in image processing, machine vision and pattern-recognition to intelligently detect fire in a manner like the way humans sense fire.

Conventional methods have proven to be inefficient and unreliable in many applications and this could be attributed to many reasons, such as proximity of sensors to the source of the fire – to reduce transport delay. In addition, they are oftentimes difficult to use in places with excessive ceiling heights or large areas such as warehouses, tunnels, and outdoors. They are also not suitable in harsh environments and in areas with strong airflow-since the air flow may easily dilute the concentration of the smoke.

Video-based Fire Detection (VFD) techniques detect fire by recognizing either smoke or flame anywhere within the field of view of the camera at a distance by using numerical analysis to model the monitored area [13]. Vision-based detection techniques can be used to sense the presence of flames within the camera's field of view, reflected fire light when flames are covered, presence of ambient or pluming smoke clouds, and intrusion into monitored property. VFD techniques are becoming

viable alternatives to the conventional fire detection methods and have shown to be useful in solving several problems associated with conventional fire sensors [1]. VFD techniques have numerous advantages such as fast response, indoor and outdoor detection at a distance, non-contact, absence of spatial limits, ability to provide fire progress information, and forensic evidence for fire investigations [13].

Currently, available VFD algorithms mainly use models that are trained with observable characteristics of flame or smoke. In early studies, flame detection was the main subject of investigation. Recently, more attention is being focused on smoke detection. This is because smoke is usually produced before flames and can readily be observed from a long distance; therefore, it is an important sign for early fire detection [2].

Many smoke detection algorithms using video images captured in visible-spectrum have been proposed [3-13]. These algorithms extract structural and statistical features from visual signatures such as motion, colour, edge, obscuration, disorderliness, growth rate, contour, geometry, texture and energy of smoke regions. The extracted features are then used as inputs for rule-based, Bayesian, or rule-first-Bayesian-next analysis to detect the presence of smoke. A survey of different methods used for smoke detection is discussed in our earlier study [13]. [9] proposed a wavelet-based real-time smoke detection algorithm, in which both temporal and spatial wavelet transformations were employed. The temporal wavelet transformation is used to analyse the flicker of smoke like objects, while the spatial wavelet transformation is implemented to calculate the decrease in high-frequency content corresponding to edges caused by the blurring effect of smoke. [10] proposed a method targeted at reducing the false alarms of the smoke detection systems in their previous works. The smoke is represented as a texture using the parameters obtained from background estimation, wavelet transform, and colour information. The model is trained using SVM, and promising simulation results were obtained. [12] proposed a smoke-detection approach that utilizes block-based spatial and temporal analyses. A candidate-region extraction step is firstly performed using a combination of temporal difference and GMM background subtraction techniques. Then, the method extracts energy-based and normalized-RGB colour-based features within the spatial, temporal, and spatial-temporal wavelets domains [13]. The three features are combined and fed to a Gaussian kernel-based SVM for classification. To reduce the false alarm rate and maintain a high detection rate with a short reaction time, a temporal-based alarm decision unit (ADU) is introduced. An average detection rate of 83.5 %, false-alarm rate of 0.1% with average reaction time of 1.34 seconds was reported.

Smoke detection has been recognized as part of dynamic texture (DT) segmentation. Nonetheless, DT segmentation is very challenging due to their unknown spatiotemporal extension and stochastic nature of the motion fields. Leveraging on the remarkable results obtained by researchers in dynamic textures segmentation, [2] proposed feature extraction methods that exploit dynamic characteristics of smoke for video-based smoke detection [13]. The algorithm is made up of various block-based processing stages which include candidate smoke blocks detection using motion and colour in RGB colour space; and candidate smoke blocks verification using accumulative motion orientation, Histograms of Equivalent Patterns (HEP)-based spatial texture descriptors, and Space-time Feature Analysis which consists of inter-frame difference and dynamic texture Descriptors on Three Orthogonal Planes [13]. They carried out extensive comparative studies on major spatial and dynamic texture descriptors. They introduced Edge Orientation Histogram (EOH) in three orthogonal planes. The performances of the proposed features are evaluated using SVM classifiers. Their experimental results show that improved detection accuracy and false alarm resistance are achieved compared with state-of-the-art technologies.

Due to the irregular shapes of smoke, varied lighting conditions, occlusions, shadows, scene complexity, video-based smoke detection remains a challenging task. This study proposes an effective smoke-detection method using spatial-temporal wavelet energy analyses and Weber Local Descriptor in three orthogonal planes (WLD-TOP) as dynamic texture descriptor. In this paper, we introduce a novel method for smoke detection that exploits variations in wavelet energy of a scene covered with smoke and dynamic textural properties of smoke. [16] demonstrated that WLD outperforms in texture recognition than state-of-the-art best descriptors like LBP, Gabor, and SIFT. The basic WLD descriptor is a histogram where differential excitation values are integrated according to their gradient orientations. In this study, we generalize the spatial mode of WLD to a spatiotemporal mode as it was done in previous studies whereby LBP was generalized as a spatiotemporal descriptor, i.e., LBP in three orthogonal planes (LBP-TOP), which is very promising in DTs recognition. Likewise, we refer to the spatial-temporal mode of WLD as WLD-TOP.

The rest of the paper is organized as follows. The methodology used for the Smoke Detection system is discussed in Section 2. Experimental results are presented in Section 3. Section 4 concludes the paper.

2. Methodology

2.1. VSD System Architecture

The proposed Video-based Smoke Detection (VSD) system uses a combination of attributes (motion, colour, energy and texture) whose mutual occurrence leaves smoke as their only combined possible cause; and detect smoke using SVM classifier by block processing. The block diagram of the proposed VSD system is shown in Fig. 1. The architecture comprises of data acquisition, pre-processing, feature extraction, classification and post-processing stages.

2.2. Pre-Processing

The pre-processing stage comprised many sub-units which were interconnected to obtain regions that were suspected to contain smoke pixels. The sub-units in this stage were: image sub-blocking, RGB-Greyscale image conversion, colour analysis in HSI colour space, GMM background modelling and subtraction. For the purpose of model training and testing, video clips were collected from the test data previously used in [10], along with additional video clips downloaded from the following websites: http://signal.ee.bilkent.edu.tr/VisiFire/Demo/SampleClips; http://cvpr.kmu.ac.kr and http://imagelab.ing.unimore.it/visor. The frame rate of the video data varied from 15 to 30 Hz and the size of the video clips varied between 320 by 240 and 640 by 480 pixels. Brief description of the video clips used for system training and testing is shown in Table 1. Using video clips employed in previous studies allows quantitative comparison of proposed method with state-of-the-art methods in smoke detection. Since smoke is a non-rigid object, object-based image segmentation is inefficient for smoke detection in video. Therefore, a block-based technique, which provided a more effective smoke detection was used. Input images were subdivided into non-overlapping 'N by N' square blocks, and the features were extracted from these local regions for smoke detection. Generally, there is a trade-off between complexity and performance of block-based image segmentation. It was observed that as the number of sub-blocks increased, the classification accuracy improved. However, the computational cost and the complexity of the detection also increased. The block size of 16 by 16 pixels was found to be a good compromise between accuracy and complexity. Video clips with frame height or width that were not multiple of 16 were padded by repeating border elements of the frame to make the frame height and width to be a multiple of 16. Sub-blocking was followed by a moving-block detection algorithm implemented using Gaussian Mixture Models (GMM). The video frames were then transformed into HSI colour space, where further analyses were performed to differentiate smoke candidate blocks from other non-smoke moving blocks. Smoke is semi-transparent when it initially starts to expand, which leads to a decrease in the chrominance values of pixels. YUV, YCbCr, HSV and HSI colour spaces were investigated on smoke of different colours to find robust colour model that will adequately characterize smoke of different colours with low computational complexity. Since smoke may have any colour (which can be grey, light grey, white, dark grey or black) depending on compositions of the fuel material, the chrominance based methods were found to be inadequate for smoke detection. HSI colour space was used for the proposed VSD as it provided colour-invariant characteristic feature that reliably differentiated smoke from other moving objects. Every pixel in each block was transformed from RGB colour space to HSI colour space using Eq (1) to (3). Every frame in a video sequence was multiplied by the foreground mask obtained from GMM. Saturation (S) and Intensity (I) were obtained from the resulting frame. A pixel is considered to be a smoke candidate if its saturation and intensity were less than empirically determined thresholds. A binary mask, (Colour_Motion_mask), was then obtained which indicated whether a given pixel was a smoke candidate or not. Since the Hue component of HSI was not required in this analysis, only Saturation and Intensity were computed to reduce computational complexity of the smoke detection system. The Colour_Motion_mask, $\varphi_{(i,j)}$ is defined by Eq (4).

Hue, H is given as

$$H = \begin{cases} \theta, & \text{if } B \leq G \\ 360 - \theta, & \text{if } B \geq G \end{cases} \quad (1)$$

where $\theta = \cos^{-1}\left\{\frac{0.5[(R-G)+(R-B)]}{[(R-G)^2+(R-B)(G-B)]^{\frac{1}{2}}}'\right\}$

Saturation, S is given as

$$S = 1 - \frac{3}{R+G+B}[\min(R, G, B)] \quad (2)$$

while intensity, **I** is given as

$$I = \frac{(R+G+B)}{3} \quad (3)$$

$$\Phi_{(i,j)} = \begin{cases} true & if\ S_{(i,j)} < S_{Thresh}\ and\ I_{(i,j)} < I_{Thresh} \\ false & otherwise \end{cases} \quad (4)$$

The flowchart for the HSI colour analysis of moving block is shown in Fig. 2.

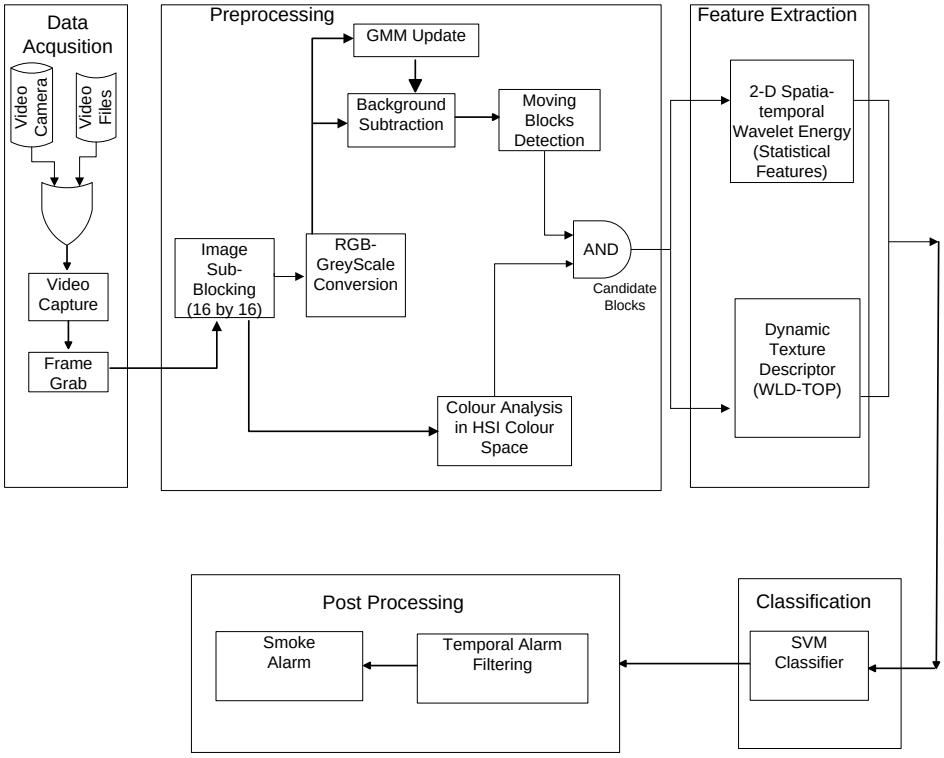

Fig. 1 The VSD Architecture.

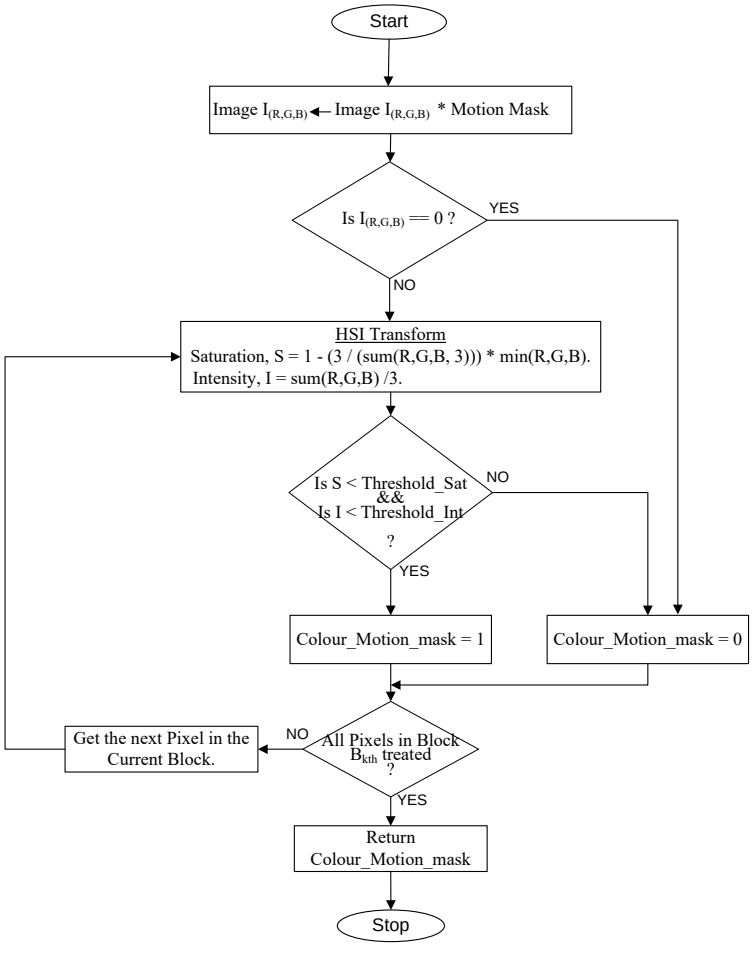

Fig. 2 Flowchart of the HSI Colour Analysis of a Moving Block.

Table 1 Brief description of the video clips used for system training and testing.

Video Sequence	Source	Description	Frame Rate
Movie 1	http://signal.ee.bilkent.edu.tr/VisiFire/Demo/SampleClips/ swindow.avi	Burning truck	25
Movie 2	http://imagelab.ing.unimore.it/visor/ smoky.avi	Smoke from fire in a garden	30
Movie 3	http://signal.ee.bilkent.edu.tr/VisiFire/Demo/SampleClips/swastebaket.avi	Smoke from burning cotton rope	25
Movie 4	http://cvpr.kmu.ac.kr/movmt.avi	People walking outside	15
Movie 5	http://www.firesense.eu./black_smoke.avi	Black smoke from burning tire	25
Movie 6	http://signal.ee.bilkent.edu.tr/VisiFire/Demo/SampleClips/sbehindthefence	Fast-moving smoke with a pedestrian	15
Movie 7	Obtained using camera in an outdoor scene	Burning foam mattress	25
Movie 8	www.HDNatureFootage.com/trucks.mov	Gray-coloured moving truck	30
Movie 9	www.HDNatureFootage.com/rhinos.avi	Two rhinos walking outside	25
Movie 10	www.HDNatureFootage.com/men.mp4	Three men walking in a hallway	15
Movie 11	http://signal.ee.bilkent.edu.tr/VisiFire/Demo/SampleClips/ Sparkinglot.avi	Crowded parking lot	15
Movie 12	http://signal.ee.bilkent.edu.tr/VisiFire/Demo/SampleClips/ carlight2.avi	Light smoke in a tunnel with pedestrians	30
Movie 13	Obtained using camera in a poorly-lit room	Candle Smoke in a room	30
Movie 14	http://signal.ee.bilkent.edu.tr/VisiFire/Demo/SampleClips/ carlight2.avi	Cars in a tunnel at night	25
Movie 15	http://cvpr.kmu.ac.kr/forest_smoke.avi	Light smoke in a forest fire	15
Movie 16	Obtained using camera in an outdoor scene	Moving cloud in a forest	15
Movie 17	www.HDNatureFootage.com/ocean_wave.mov	Ocean wave	30
Movie 18	http://www.firesense.eu./ sparkinglot.avi	Smoke from fire in a parking lots	25
Movie 19	Obtained using camera in an outdoor scene	Fast moving cars on a tarred road	30

Pixels with the maximum number of changes across frames were selected from a large number of video sequences (smoke and non-smoke video clips). Saturation and Intensity values were computed for the selected pixels in each frame of the sequences. The results obtained for the selected pixels in a typical smoke video clip and non-smoke video clip are shown in Fig. 3(a to d). From the result, it was observed that variations in intensity and saturation of smoke pixels are significantly different from those of other moving objects. While variations in smoke pixels are gradual and irregular, that of rigid moving objects tends to be spontaneous and regular. The gradual and irregular nature of variations in intensities of smoke pixels could be attributed to irregular nature of smoke motion. Also, in the absence of strong wind, the intensity of smoke pixels varied slowly when compared with that of a pixel of a non-smoke solid moving object.

As shown in Fig. 3(a) and Fig. 3(c), saturation values of the selected smoke pixel varied between 0.061 and 0.318; while that of the selected non-smoke moving pixel varied between 0.005 and 0.19. The results indicated that a smoke pixel could not have zero value -since saturation of zero value could only be obtained from objects with pure black colour. Though the minimum and maximum saturation values obtained for the selected non-

smoke moving pixel were 0.005 and 0.19 respectively, it should be noted that the saturation value of a non-smoke pixel could vary between 0.000 (for pure black object) and 1.000 (for pure white object). To reduce the possibility of categorizing a smoke pixel as non-smoke a threshold value of 0.7 was selected for maximum saturation value that could be obtained from smoke pixel. As shown in Fig. 3(b) and Fig. 3(d), it was observed that the intensity values of the selected smoke pixel varied between 0.319 and 0.616 while that of selected non-smoke object varied between 0.290 and 0.990. The intensity value of an ordinary non-smoke object can range from 0.000 (for black object) to 1.000 (for shining white object). Though the maximum intensity value of the selected smoke pixel was 0.616, a threshold value of 0.900 was used to differentiate smoke pixel from other moving objects. This was important to reduce the possibility of rejecting a smoke candidate pixel at the pre-processing stage. Though the selected threshold allowed other non-smoke blocks to pass the pre-processing stage, the non-smoke blocks were easily rejected during SVM classification.

Thus, in generating colour mask, a moving pixel was considered to be smoke candidate if its saturation was less than 0.7 and its intensity less than or equal to 0.9. An "AND" logical combination of the colour mask and motion mask was performed to obtain smoke candidate blocks that were fed to the feature extraction stage.

2.3. Feature Extraction

The input data (smoke candidate blocks in the video frame) was transformed into a reduced representation set of features at this stage. The outputs (marked blocks) of the pre-processing stage were used as the inputs for the feature extraction stage. Two processes used in this stage were 2-D spatial-temporal wavelet analysis and dynamic texture analysis.

2.3.1. 2-D spatial-temporal wavelet analysis.

Previous studies have shown that wavelet sub-images contain the spatial texture and edge information of the original image in form of local extrema. Discrete Wavelet Transform (DWT) has become an efficient tool in evaluating the energy variation of an intensity image for smoke detection [8]. DWT has also proved useful in obtaining decomposed images through various sub-bands that allow extraction of smoke's features at different resolutions and frequencies. The two-dimensional DWT is made up of approximation and detail parts. The original image is decomposed into four sub-images, which are W_{ϕ}, W_{φ}^{H}, W_{φ}^{V} and W_{φ}^{D}. The scale j + 1 approximation coefficients are again divided into four sub-images of smaller size. In other words, the output of DWT is a vector of the form $[A_n, (H_j, V_j, D_j)_{j = 1,..., n}]$ where A_n is a low-resolution approximation (low-frequency data of row and column, LL) of the original image, H_j is wavelet sub-image containing the image details in horizontal direction (high-frequency data of row and low-frequency data of column, HL), V_j is wavelet sub-images containing the image details in vertical direction (low-frequency data of row and high-frequency data of column, LH) , D_j is wavelet sub-image containing the image details in diagonal direction (high-frequency data of row and column, HH) at the j-level decomposition. The output of n-level DWT decomposition on the original image will produce 3n + 1 sub-images. A 1-level 2D decomposition is shown in Fig. 4.

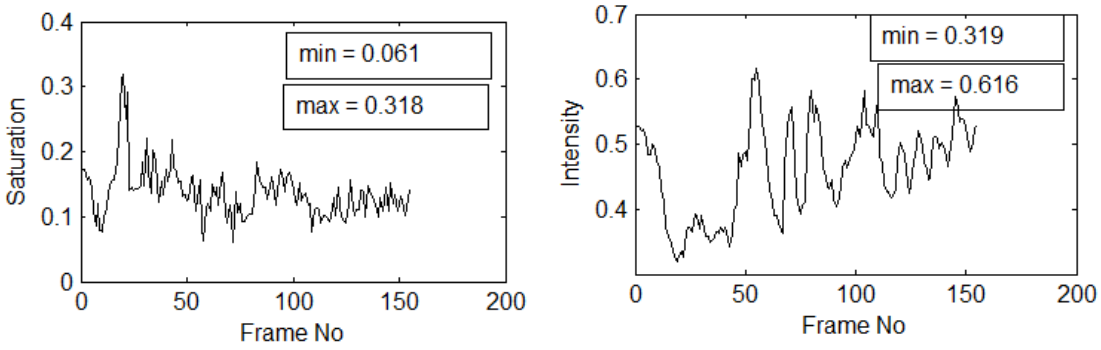

(a) Saturation variation (b) Intensity variation

Fig. 3 Saturation and intensity variation of selected pixels of video frames with smoke.

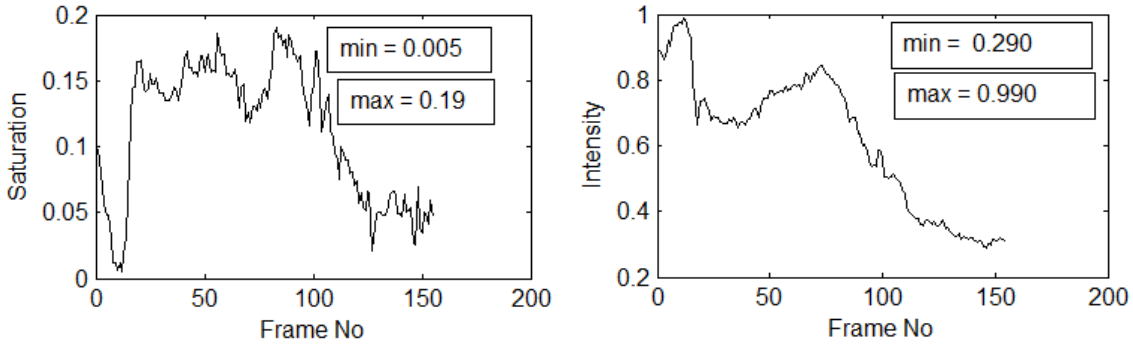

(c) Saturation variation (d) Intensity variation

Fig. 3 Saturation and intensity variation of selected pixels of non-smoke video frames.

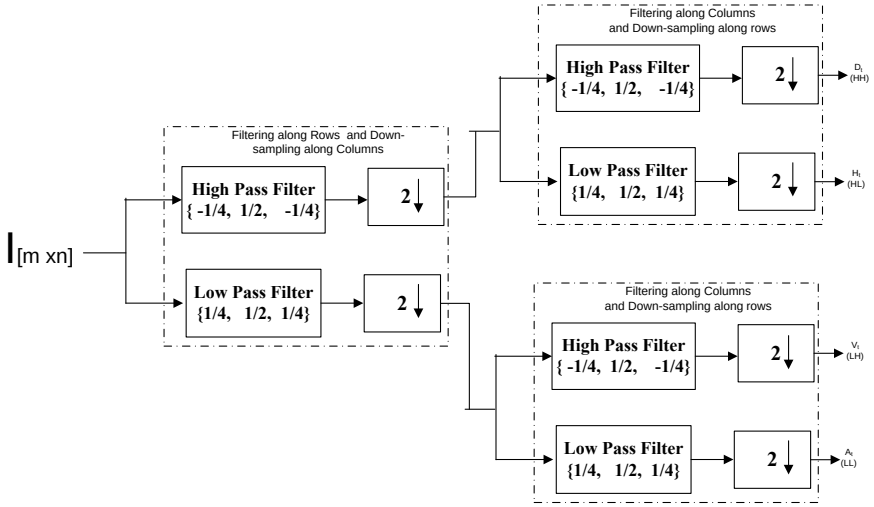

Fig. 4 2-D Discrete wavelet transform.

High-frequency energy of each block was computed using single stage 2-D discrete wavelet decomposition of the current image block using Eq (5).

$$(I_t, b_k) = \sum_{m,n\ j\ \epsilon\ b_k} H_t^2(m,n) + V_t^2(m,n) + D_t^2(m,n) \quad (5)$$

where b_k is the kth block of the active frame and I_t is the input image at time t; H, V and D are vertical, horizontal and diagonal sub-band details respectively.

One-level Daubechies (Haar) wavelet was used for the wavelet analysis. To extract spatial-temporal energy variations from video frames, wavelet energy was computed for W consecutive video frames and five derived features were calculated from the sub-band energies. The five statistical parameters were variance, standard deviation, skewness, kurtosis and sum of inter-frame energy differences.

Blocks with maximum temporal variation across frames were selected from a smoke video clip and non-smoke video clip. Each block's energy was computed over the video sequences. Fig. 5 shows the results of a comparison of the energy analysis for smoke and an ordinary moving object. Smoke produced a smoother variation in the energy value. In contrast, non-smoke solid moving objects produced large instantaneous variations in the energy value. To obtain these variations irrespective of the absolute value of the block energy, several statistical parameters were computed. The computed parameters were: variance, standard deviation, skewness, kurtosis and sum of inter-frame energy differences.

Fig. 5(a) and 5(b) show that changes in variance of wavelet energy produced when a selected block was obscured by smoke were more irregular than when a selected block was obscured by non-smoke moving objects. The variance of wavelet energy in the case of non-smoke moving block was predictably regular and varied from near zero to maximum value along the consecutive video frames. Fig. 5(c) and 5(d) show the plot of sum of energy change for the selected block in smoke and non-smoke block respectively over time. It could be observed that the sum of energy change for non-smoke moving objects exhibits more predictable, regular and oscillatory change than that of smoke. From the results, all the statistical parameters obtained from wavelet energy analysis were relevant in discriminating smoke from other moving objects.

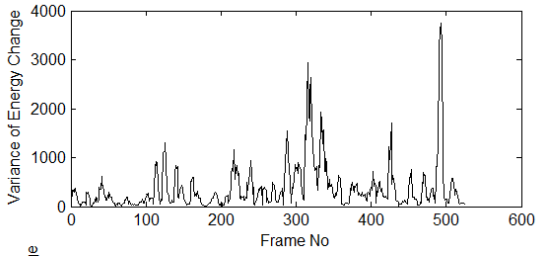

Fig. 5(a) Variance of energy change for selected block in video with smoke.

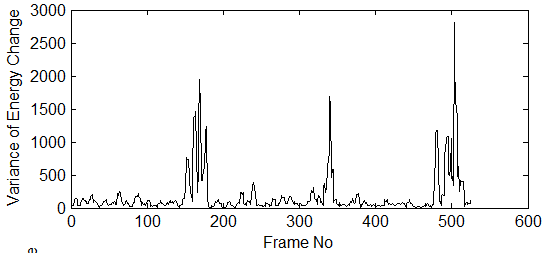

Fig. 5(b) Variance of energy change for selected block in non-smoke video.

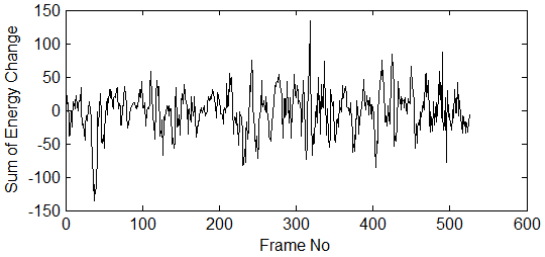

Fig. 5(c) Sum of energy change for selected block in video with smoke.

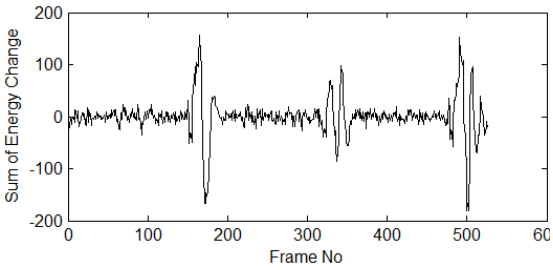

Fig. 5(d) Sum of energy change for selected block in non-smoke video.

The results obtained showed that the spatial-temporal features obtained from wavelet energy of a video clip could easily be used to distinguish smoke from non-smoke moving object.

2.3.2. Dynamic Texture analysis using Weber Local Descriptor (WLD)

Weber Local Descriptor (WLD) descriptor is based on Weber's Law which states that the change of a stimulus (such as sound or light) that is just noticeable is a constant ratio of the original stimulus. Inspired by this law, [16] proposed WLD descriptor for texture representation. WLD descriptor represents an image as a histogram of differential excitations and gradient orientations and possesses several desirable properties such as robustness to noise and illumination changes, elegant detection of edges and powerful image representation [16]. WLD is computationally simple and effective for texture classification, and it is complementary to LBP. Three steps which are required in computing basic WLD descriptor are: finding differential excitations, gradient orientations and building the histogram.

To get differential excitation $\mathcal{E}(x_c)$ of a pixel x_c, firstly the intensity differences of x_c with its neighbours x_i, $i = 1, 2, \ldots, p$ are calculated as

$$\Delta I_i = I_i - I_c \quad (6)$$

Then the ratio of total intensity difference of x_c with its neighbours x_i to the intensity of x_c is calculated as follows:

$$f_{ratio} = \sum_{i=0}^{P-1}\left(\frac{\Delta I_i}{I_c}\right) \quad (7)$$

Arctangent function can be used as a filter on f_{ratio} to enhance the robustness of WLD against noise which results in:

$$\varepsilon(x_c) = \tan^{-1}\left[\sum_{i=0}^{P-1}\left(\frac{\Delta I_i}{I_c}\right)\right] \quad (8)$$

The resulting differential excitation $\varepsilon(x_c)$ may be positive or negative. The positive value indicates that the current pixel is darker than its surroundings and negative value means that the current pixel is lighter than the surroundings. Next main component of WLD is gradient orientation. For a pixel x_c the gradient orientation is computed as follows:

$$\theta(x_c) = \tan^{-1}\left[\frac{I_{xx}}{I_{yy}}\right] \quad (9)$$

where I_{xx} is the intensity difference between two pixels on the left and right of the current pixel x_c, and I_{yy} is the intensity difference of two pixels directly below and above the current pixel, $\theta \in \left[-\frac{\pi}{2}, \frac{\pi}{2}\right]$

The gradient orientations are quantized into T dominant orientations as:

$\phi_t = \frac{2t}{T}\pi$;

where

$$t = \mathrm{mod}\left(\left\lfloor\frac{\theta'}{2\pi/T} + \frac{1}{2}\right\rfloor, T\right) \quad (10)$$

In our case T = 12 and the dominant orientations are

$$\phi_t = \frac{t\pi}{4},\ t = 0, 1, ...,T-1; \quad (11)$$

Thus, all orientations located in the interval

$$[\phi_t - \left(\frac{t\pi}{4}\right), \phi_t + \left(\frac{t\pi}{4}\right)] \quad (12)$$

are quantized as ϕ_t. WLD descriptor is then subsequently built from the calculated differential excitation and dominant orientation. Corresponding to each dominant orientation, ϕ_t: t = 0, 1, 2, …, T-1 differential excitations are organized as a histogram H_t.

2.3.3. Spatial-Temporal WLD Descriptor

To exploit dynamic textual properties of smoke, we use WLD-TOP as a local spatial-temporal texture descriptor. WLD-TOP is a spatial-temporal descriptor which computes the WLD feature in three orthogonal planes as shown in Fig. 6. Fig. 6(a) is a sequence of frames (or images) of a DT; 6(b) denotes the three orthogonal planes or slices XY, XT and YT, where XY is the appearance of DT; XT shows the visual impression of a row changing in temporal space; and YT describes the motion of a column in temporal space; 6(c) illustrates the vertex coordinates of the three orthogonal planes for the feature computation of WLD of one pixel; 6(d) shows how to compute sub-histograms from three slices which are denoted as WLD_{XY}, WLD_{XT} and WLD_{YT}.

The WLD-TOP descriptor's underlying framework is shown in the flowchart in Fig. 7. The operator extracts differential excitation and gradient orientation of every pixel in a marked image block using its 3 by 3- spatial-temporal (XY, XT, YT) neighbourhood. This implies a circle of radius R = 1.0 from the centre pixel, and 8 sampling points on the edge of this circle were taken and compared with the value of the centre pixel.

WLD-TOP descriptors were extracted from 30,000 pre-processed blocks obtained from smoke and non-smoke video clips. The scatter plot of the results obtained is presented in Fig. 8. The x-axis indicates the number of bins; while the y-axis is the mean value of normalized histogram which counts the number of patterns that fall into each bin from blocks of smoke and non-smoke blocks. From the results, WLD-TOP descriptors provide good discriminatory ability for separating smoke blocks from non-smoke blocks.

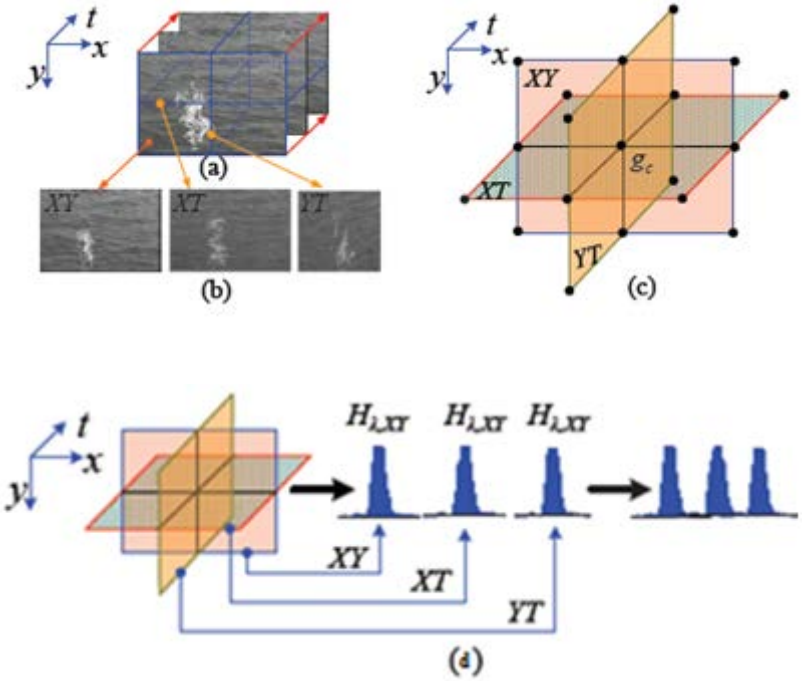

Fig. 6 Three planes in spatial-temporal domain to extract TOP features, and the histogram concatenated from three planes. (a) Image frames, (b and c) the x-y, y-t, and x-t planes, and (d) concatenation of resulting histograms into a single feature set [17].

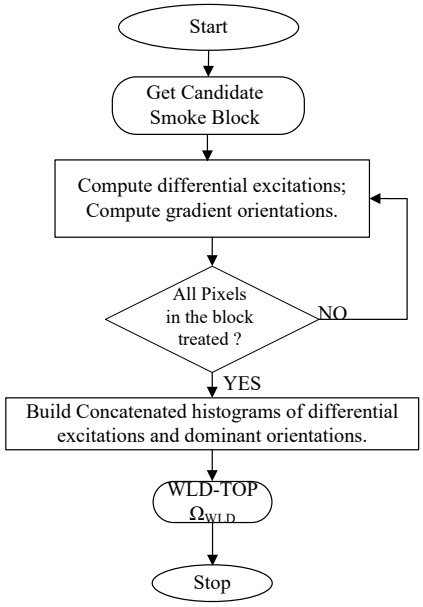

Fig. 7 Flowchart of major steps in extracting (WLD-TOP) as dynamic texture descriptor.

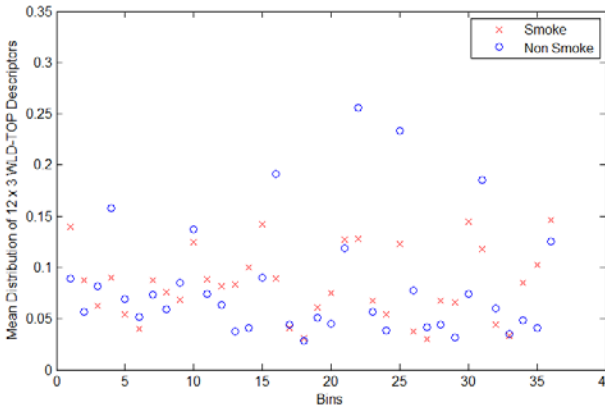

Fig. 8 Probability Distribution of WLD-TOP at (P, R) = (8,1) of Smoke and non-Smoke blocks.

2.4. Classification

Support Vector Machine (SVM) was used for training and testing of the model on the extracted feature vectors. Gaussian radial basis function was used in training and testing of the model. The size of feature sets generated from smoke and non-smoke video clips were usually very large, and this was computationally intensive for SVM model training – especially when tuning the model for the best combination of parameters. The feature sets were thus sub-sampled using Random Sampling. Different parameters were tried, using unconstrained nonlinear optimization technique, for training, and checked via 10-fold cross-validation to obtain the best parameters. The values of SVM parameters (RBF sigma, σ and misclassification penalty, ς) obtained for sub-samples were used to model SVM on feature sets extracted from 15,000 feature vectors of smoke and 15,000 feature vectors of non-smoke moving blocks. Ten-fold cross-validations were performed on the feature sets to avoid over-fitting. The SVM model structure obtained from the modelling was saved in a file for subsequent smoke detection.

2.5. Post-Processing

To reduce false alarm, after candidate smoke blocks have been classified, they were fed to post-processing stage for further verification. Statistical smoke alarm data was obtained from frame to frame. The number of alarms in each block was computed over five consecutive video frames. If the value was greater than two, a real alarm was generated.

2.6. Performance Evaluation

Accuracy, Detection Rate (DR), False Alarm Rate (FAR) and Precision were used to evaluate the performance of the system.

$$\text{Accuracy}\ (\%) = \frac{\text{TP} + \text{TN}}{\text{TP} + \text{TN} + \text{FP} + \text{FN}} \times 100\% \quad (13)$$

$$\text{DR}\ (\%) = \frac{\text{TP}}{\text{TP} + \text{FN}} \times 100\% \quad (14)$$

$$\text{FAR}\ (\%) = \frac{\text{FP}}{\text{TN} + \text{FP}} \times 100\% \quad (15)$$

$$\text{Precision}\ (\%) = \frac{\text{TP}}{\text{TP} + \text{FP}} \times 100\% \quad (16)$$

where TP, TN, FP, and FN represent True Positive, True Negative, False Positive, and False Negative respectively.

2.7. Implementation

The algorithm was implemented in MATLAB 8.1.0.604 (R2013a) on a computer with Pentium (R) Dual-Core 2.20 GHz CPU and 2GB RAM. Graphic User Interfaces (GUIs) were built to make utilization of developed functions to be user friendly. Using MATLAB's 'GUIDE', three Graphical User Interfaces were developed to simplify the usage of developed VSD.

3. Results

A total of 19 video clips were used from which 30,000 blocks were generated to obtain feature sets for VSD modeling and testing. WLD-TOP without Wavelet Energy has 0.0362 s as average extraction time, while WLD-TOP with Wavelet Energy has average extraction time of 0.0376 s. Average time taken was 0.0019 s to classify WLD-TOP with

Wavelet Energy. As shown in Table 2, accuracy of 99.30% and detection rate of 99.28% were obtained using WLD-TOP with Wavelet Energy, while the lower accuracy of 99.10% was obtained from WLD-TOP without Wavelet Energy. Table 3 shows the feature extraction and recognition time using different feature sets.

The proposed VSD system was tested on several video clips of different scenarios. The developed VSD system achieved perfect detection results when tested on video clips from outdoor and indoor environmental situations with presence and absence of other non-smoke moving objects. Fig. 9 (a to f), show the performance of the developed VSD when tested on video clips of smoke in indoor environment, smoke in outdoor environment with other moving objects, smoke in outdoor environment with strong wind and non-smoke moving objects in outdoor environment. Red blocks indicate smoke regions while blue blocks indicate non-smoke moving region. The proposed system successfully generated alarm for smoke events in every test video. However, there were instances when the proposed system showed a very small number of false alarms as shown in Fig. 9 (c).

The developed method was compared with other recent approaches, including the Spatial-Temporal Wavelet Analyses method proposed by [12]; and Histograms of Equivalent Patterns and Space-time Analysis method proposed by [2]. Table 4 shows a comparison of the results with the earlier smoke-detection methods. Using false alarm rate and detection rate or accuracy as performance evaluation metrics, the proposed method WLD-TOP+W showed improvement in performance when compared to methods in previous studies.

4. Conclusion

Algorithm for smoke detection in video were developed using effective combination of spatial and temporal features computed from wavelet energy and dynamic texture analysis. Moving blocks in

Table 2 SVM model performances obtained for different feature sets.

Dynamic Texture Descriptor	Support Vector Dimension	SVM Σ	Ϛ	Accuracy %	DR %	FAR %
WLD-TOP + WE	44	3.5724	1.5583	99.30	99.28	0.65
WLD-TOP	36	3.6036	1.1929	99.20	99.10	0.70

Table 3 Feature Extraction and Recognition time using different feature sets.

Dynamic Texture Descriptor	Support Vector Dims	Extraction Time (s)	Recognition Time (s)
WLD-TOP with Wavelet Energy.	44	0.0376	0.0019
WLD-TOP.	36	0.0362	0.0016

Table 4 Comparison with existing works.

Method	Features	Classifier	Accuracy	DR %	FAR %	Precision %
Smoke Detection using Spatial and Temporal Analyses [12]	2-D Spatial Wavelet Analysis	SVM (RBF)	--	93.5	38.0	--
	1-D Spatial-temporal Energy Analysis	SVM (RBF)	--	91.7	13.1	--
	1-D Temporal Chromatic Configuration Analysis	SVM (RBF)	--	85.5	11.2	--
Early Fire Detection Using HEP and Space-time Analysis [2]	EOH-TOP (with resolution of 48 bins)	SVM (RBF)	97.3511	--	--	--
	Uniform LBP-TOP	SVM (RBF)	97.4007	--	--	--
WLD-TOP +W (Proposed Method)	WLD-TOP	SVM (RBF)	99.20	99.10	0.70	99.30
	WLD-TOP + Wavelet Energy	SVM (RBF)	99.30	99.28	0.65	99.74

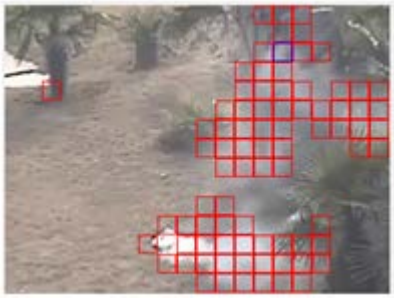

(a) Smoke in outdoor environment

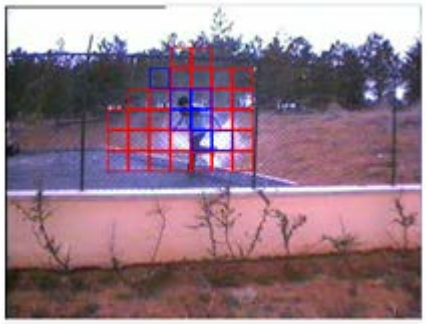

(b) Smoke in outdoor environment with strong wind

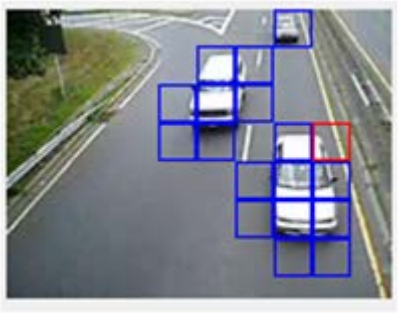

(c) Non-Smoke moving object in moving objects

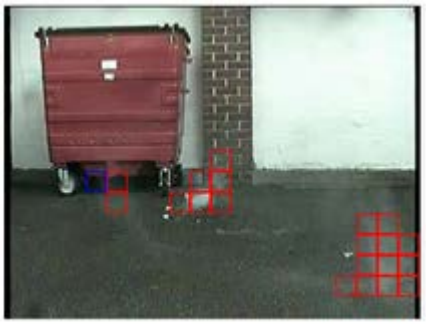

(d) Smoke in semi-outdoor outdoor environment

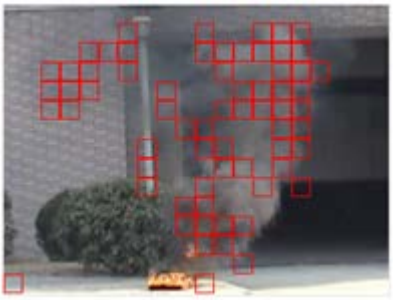

(d) Smoke in outdoor environment

(f) smoke in indoor environment

Fig. 9 Performance of the developed VSD tested on video clips.

video frames were firstly segmented and analysed in HSI colour space. Wavelet energy analyses were then performed on smoke candidate blocks. Weber Local Descriptors in Three Orthogonal Planes (WLD-TOP) were also obtained from candidate smoke block. Features extracted from energy analyses were separately combined with WLD-TOP and used as inputs to Support Vector Classifier with radial based kernel function. The algorithm was implemented in MATLAB 8.1.0.604 (R2013a). Using accuracy, precision, detection rate and false-alarm rate as metrics for performance evaluation, it was observed that the combined features produced good results. The following results were obtained for accuracy, precision, detection rate and false alarm rate respectively, 99.30 %, 99.74 %, 99.28 % and 0.65 %.

5. Future Works

Future research work on video-based smoke detection will consider efficient method for extracting WLD-TOP at increased histogram resolution. This will not only reduce the response time of the system, it will also increase the effectiveness of the proposed system

Competing interests

The authors have declared that no competing interests exist.

References

[1] E.A. Çetin, K. Dimitropoulos, B. Gouverneur, H.Y. Habiboglu, B.U. Töreyin, and S. Verstockt, et al., "Video fire detection – review," Digital Signal Processing, vol. 23, no. 6, pp. 1827–1843, 2013.

[2] J. Chen and Y. You, "Early Fire Detection Using HEP and Space-time Analysis," Computer Vision and Pattern Recognition (cs.CV); Multimedia (cs.MM) arXiv:1310.1855, pp. 228 –312, 2013.

[3] J. Chen, Y. You, and Q. Peng, "Dynamic analysis for video-based smoke detection," International Journal of Computer Science Issues, vol. 10, no. 2, pp. 298–304, 2013.

[4] L. Wen-hui, F. Bo, C. Xiao-lin, W. Ying, and L. Pei-xun, "A Block-based Video Smoke Detection Algorithm," Journal of Jilin University (Science Edition), vol. 50, no. 5, pp. 979-986, 2012.

[5] J. Gubbi, S. Marusic, and M. Palaniswami, "Smoke detection in video using wavelets and support vector machines," Fire Safety Journal, vol. 44, no.8, pp. 1110 –1115, (2009).

[6] R.A. Gonzalez-Gonzalez, V. Alarcon-Aquino, O. Starostenko, R. Rosas-Romero, J.M. Ramirez-Cortes, and J. Rodriguez-Asomoza, "Wavelet-based smoke detection in outdoor video sequences," in Proceedings of the 53rd IEEE Midwest Symposium on Circuits and Systems (MWSCAS), pp. 383 –387, 2010.

[7] F. Yuan, "A fast accumulative motion orientation model based on integral image for video smoke detection," Pattern Recognition Letters, vol. 29, no. 7, pp. 925 - 932, 2008.

[8] B. U. Töreyin, Y. Dedeoglu, and A.E. Çetin, "Wavelet-based real-time smoke detection in video," in European Signal Processing Conference (EUSIPCO), pp. 246- 302, 2005.

[9] B. U. Töreyin, Y. Dedeoglu, and A.E. Çetin, "Flame Detection in Video Using Hidden Markov Models," in International Conference on Image Processing (ICIP 2005), pp. 1230–1233, 2005.

[10] B. U. Töreyin, Fire Detection Algorithms Using Multimodal Signal and Image Analysis. PhD thesis, Dept. Elect. Eng., Bilkent University, Ankara, Turkey. Available at: http://www.arehna.di.uoa.gr/thesis/uploaded_data/Fire_Detection_Algorithms_Using_Multimodal_Signal_and_Image_Analysis_2009_thesis_1232106137.pdf, 2009.

[11] P. Piccinini, S. Calderara, and R. Cucchiara, "Reliable smoke detection system in the domains of image energy and colour," in Proceedings of International Conference on Image Processing, pp. 1376 –1379, 2008.

[12] L. Chen-Yu, L. Chin-Teng, H. Chao-Ting, and S. Miin-Tsair, "Smoke Detection using Spatial and Temporal Analyses," International Journal of Innovative Computing, Information and Control, vol. 8, no. 6, pp. 200-300, 2012.

[13] J.A. Ojo and J.A. Oladosu, "Video-based Smoke Detection Algorithms: A Chronological Survey," International Institute for Science, Technology and Education (IISTE), ISSN 2222-1719 (Paper), ISSN 2222-2863 (Online) vol. 5, no. 7, 2014.

[14] B.U. Töreyin, Y. Dedeoglu, A.E. Çetin, S. Fazekas, D. Chetverikov, and T. Amiaz, et al., "Dynamic texture detection, segmentation and analysis," Proceedings of ACM International Conference on Image and Video Retrieval (CIVR), pp. 131 –134, 2007,

[15] B.U. Töreyin and A. E. Çetin, "Wildfire detection using LMS based active learning," in Proceedings of the IEEE International Conference on Acoustics, Speech and Signal Processing, pp. 12-100, 2009.

[16] U. Ihsan, H. Muhammad, M. Ghulam, A. Hatim, B. George, and M. M. Anwar, "Gender Recognition from Face Images with Local WLD Descriptor," IWSSIP 2012, Vienna, Austria, vol. 5, no.6, pp. 11-13, 2012.

[17] D. Sloven, P. Renaud, and M. Michel, "Characterization and Recognition of Dynamic Textures based on 2D+T Curvelet Transform," Signal, Image and Video Processing, pp. 146-272, 2013.